

Accepted Manuscript

New 1,2,4-triazole-based azo-azomethine dye. Part III: synthesis, characterization, thermal property, spectrophotometric and computational studies

Malihe Erfantalab, Hamid Khanmohammadi

PII: S1386-1425(14)00134-6
DOI: <http://dx.doi.org/10.1016/j.saa.2014.01.113>
Reference: SAA 11599

To appear in: *Spectrochimica Acta Part A: Molecular and Biomolecular Spectroscopy*

Received Date: 24 October 2013
Revised Date: 7 January 2014
Accepted Date: 22 January 2014

Please cite this article as: M. Erfantalab, H. Khanmohammadi, New 1,2,4-triazole-based azo-azomethine dye. Part III: synthesis, characterization, thermal property, spectrophotometric and computational studies, *Spectrochimica Acta Part A: Molecular and Biomolecular Spectroscopy* (2014), doi: <http://dx.doi.org/10.1016/j.saa.2014.01.113>

This is a PDF file of an unedited manuscript that has been accepted for publication. As a service to our customers we are providing this early version of the manuscript. The manuscript will undergo copyediting, typesetting, and review of the resulting proof before it is published in its final form. Please note that during the production process errors may be discovered which could affect the content, and all legal disclaimers that apply to the journal pertain.



New 1,2,4-triazole-based azo-azomethine dye. Part III: synthesis, characterization, thermal property, spectrophotometric and computational studies

Malihe Erfantalab and Hamid Khanmohammadi*

Faculty of science, Department of chemistry, Arak University, Arak, 38156-8-8349, Iran

Abstract

A new 1,2,4-triazole-based azo-azomethine compound, **H₂L**, has been prepared by condensation reaction of 1-(3-Formyl-4-hydroxyphenylazo)-4-ethylbenzene with prepared triazole-based diamine. The structure of **H₂L** was characterized by using FT-IR, UV-Vis and ¹H NMR spectroscopic methods as well as elemental analysis. Hard model chemometrics method has been used to determine the formation constants of zinc(II), copper(II), nickel(II) and cobalt(II) complexes of **H₂L** in DMSO by UV-Vis spectrophotometric method. Solvatochromic behavior of the dye has been also investigated in some organic solvents with different polarities. Thermal properties of the prepared dye was examined by thermogravimetric analysis. Results indicated that the framework of the dye was stable up to 245 °C. Furthermore, ¹H chemical shifts and UV-Vis of **H₂L** were studied by the gauge independent atomic orbital (GIAO), continuous set of gauge transformations (CSGT) and Time-dependent density functional theory (TD-DFT) methods respectively at the level of density functional theory using B3LYP/6-311+G(d) basis sets in DMSO. The computational data are in reasonably good agreement with the experimental data.

Keywords: Azo-azomethine; TD-DFT; 1,2,4-Triazole; GIAO; CSGT; NBO.

*Corresponding author. h-khanmohammadi@araku.ac.ir Tel: +98-861-2777401; Fax: +98-861- 4173406.

1. Introduction

Azo dyes are well-known class of organic photoactive materials due to their excellent optical switching properties, good chemical stabilities and high solution process abilities [1,2]. These materials are widely used in heat transfer printing and textile industries [3,4], optical data storage [5], switching technologies [6], photo-refractive polymer industries [7] and have been widely used in many biological reactions [8-10] and in analytical chemistry [11]. Recently, azo-azomethine dyes have also attracted increasing attention due to their interesting electronic and geometrical features in connection with their application for molecular memory storages [12], nonlinear optical elements [13], printing system [14] and biological-medical studies [15,16]. Therefore, several studies have been published on the synthesis and spectral properties of azo-azomethine dyes, as well as their transition metal complexes [17-22]. Among the plethora of new synthetic azo-azomethine dyes those containing 1,2,4-triazoles are of particular interest for several reasons. 1,2,4-Triazoles are stable compounds with rich and well-known chemistry [23-26]. The incorporation of 1,2,4-triazole into acyclic and/or macrocyclic ligands has facilitated the isolation of a wide range of transition metal complexes with interesting electrochemical and magnetic properties [27-29]. Also, their electronic properties make them suitable for surface enhanced resonance Raman scattering (SERRS) studies [30,31]. These diversified applications are at least in part a consequence of the numerous approaches that are available for the insertion of specific functionalities into the triazole nucleus.

As part of our ongoing interest in the synthesis and spectral studies of 1,2,4-triazole-based azo-azomethine dyes [25,26], we report the newly prepared azo-azomethine compounds on 1,2,4-triazole-based moiety (Figure 1) and computationally investigated their intense electric absorption band in visible region, which is decisively responsible for their color appearance. The prepared dye has been characterized by spectroscopic methods (^1H NMR,

UV–Vis and IR) as well as elemental analysis data. ^1H NMR spectrum of more stable tautomer, azo tautomer, was successfully simulated using Continuous Gauge Independent Atomic Orbitals/Density Functional Theory (GIAO/DFT) [32,33] and Continuous Set of Gauge Transformations/Density Functional Theory (CSGT/DFT) [34,35] with the B3LYP functional. Also, in order to theoretically establish the more stable tautomer in DMSO solution, we tried to assign the UV-Vis spectrum of dye by Time-dependent density functional theory (TD-DFT) [36]. The thermal property of the prepared azo dye was examined by thermogravimetric analysis which indicated that **H₂L** was stable up to 245 °C.

Figure 1

2. Experimental

2.1. Materials

All of the reagents and solvents involved in synthesis were of analytically grade and used as received without further purification. Salicylaldehyde, 4-ethylaniline, 1,3-bis(bromomethyl)benzene and hydrazine (80%) were obtained from Aldrich and Merck.

2.2. Instrumentation

The structure of all synthesized compounds was confirmed by ^1H NMR spectra, recorded on a Bruker AV 300 MHz spectrometer. FT-IR spectra were recorded as pressed KBr discs, using Unicam Galaxy Series FT-IR 5000 spectrophotometer in the region of 400-4000 cm^{-1} . Melting points were determined on Electrothermal 9200 apparatus. Thermal analysis was performed on a TGA V5.1A DuPont 2000 and Perkin-Elmer Thermogravimetric Analyzer TG/DTA 6300 instruments. C.H.N. analyses were performed on a Vario EL III elemental analyzer. Electronic spectral measurements were carried out using Agilent hp 8453 spectrophotometer in the range 300-800 nm using 1 cm path quartz cells. The measurements

were performed at 25 (± 0.5) °C. The pH measurements were made using a Metrohm 691 pH meter equipped with a glass calomel combined electrode. All calculations were performed in MATLAB 7.8 (R2009a) and Microsoft Excel 2007. Electrochemical measurements were recorded on an Autolab 30V potentiostat/galvanostat for Eco Chemicompany. All readings were taken using three electrode potentiostatic systems in DMSO with 0.1 mol cm⁻³ tetrabutylammonium perchlorate (TBAP, electrochemical grade) as supporting electrolyte. A three-electrode assembly composed of a platinum working electrode, a platinum auxiliary electrode, and Calomel reference electrode was used with sample concentrations of 1 $\times 10^{-3}$ M.

2.3. Theoretical calculations

The structure data, ¹H chemical shifts of **H₂L** and TD-DFT calculation in DMSO were calculated using Gaussian-03 [37] series of programs. A starting molecular mechanics structure for the DFT calculations was obtained using the Hyper Chem 5.02 program [38]. The geometry of the prepared compound was fully optimized at the B3LYP/6-31G* level. Vibrational frequency analyzes, calculated at the same level of theory, indicate that the optimized structure is at the stationary points corresponding to global minima without any imaginary frequency. The calculations of the computed magnetic isotropic shielding tensors were performed using GIAO/DFT [32,33] and CSGT/DFT [34,35] methods at the B3LYP/6-311++G(d) basis set. In both step of DFT and TD-DFT calculations, solvent effects of ethanol and DMSO were included using the Polarizable Continuum Model (PCM) [39]. The default Gaussian03 PCM implementation (non-equilibrium formulation) is suitably designed to predict UV/Vis spectrum described within the vertical transition scheme, where solvent polarization responds to the change of electronic distribution of the excited state molecules with the molecular orientation fixed during electronic transition. The NBO calculations [40] were performed using NBO 3.1 program as implemented in the

Gaussian 03W package at the DFT/B3LYP level in order to understand various second order interactions between the filled orbitals of one subsystem and vacant orbitals of another subsystem, which is a measure of delocalization or hyper conjugation. The second-order fock matrix was used to evaluate the donor-acceptor interactions in the NBO basis [41]. For each donor NBO(*i*) and acceptor NBO (*j*), the stabilization energy $E(2)$ associated with the *i* to *j* delocalization is estimated as

$$E(2) = \Delta E_{ij} = [q_i (F_{ij})^2] / [\epsilon_i - \epsilon_j] \quad (1)$$

Where q_i is the donor orbital occupancy, ϵ_i , ϵ_j are diagonal elements (orbital energies) and F_{ij} is the off diagonal element associated with NBO matrix.

2.4. Thermodynamic calculations

The pH of the solution (DMSO/water, 1/10 V/V) containing **H₂L** (25 mL of 5.0×10^{-5} M) was gradually adjusted in the range of 9.0 using potassium hydroxide solution. Then the absorbance spectra of the solution were recorded in wavelength range of 320–600 nm. All experiments were carried out at the temperature (25 ± 0.5) °C. Therefore, the effect of the addition of metal ions to the DMSO solution of **H₂L** was studied. The concentration of **H₂L** in DMSO was kept constant, and the metal ions were progressively added to the solution. After each addition, UV–Vis spectra of the solution were recorded.

2.5. Synthesis

2.5.1. synthesis of 1,3-bis(4-amino-3-(4-pyridyl)-5-thiomethyl-1,2,4-triazole)benzene (**L²**)

To a solution of 4-amino-3-(4-pyridyl)-5-mercapto-1,2,4-triazole (2 mmol) in aqueous ethanol (50 ml) containing KOH(2 mmol) was added 1,3-bromomethylbenzene (1 mmol). The reaction mixture was heated under reflux for 1 h. The solvent was removed in vacuo and the remaining solid was collected and washed with water (*see supporting information*). ¹H NMR(*d*₆-DMSO, ppm): 4.46(s, 4H), 6.23(s, 4H), 7.29(m, 3H), 7.56(s,br, 1H), 7.98(dd, 4H, J=6.00 Hz), 8.72(dd, 4H, J= 6.00 Hz). IR (KBr, cm⁻¹); 3334 and

3267(NH₂), 1602 (C=C, C=N), 1464, 1556 (C=C-N), 1105 (N-N). Anal. Calcd. for C₂₂H₂₀N₁₀S₂: C, 54.08; H, 4.13; N, 28.67; S, 13.13. Found: C, 54.2; H, 3.7; N, 28.3; S, 13.3.

2.5.2. synthesis of azo-azomethine dye, **H₂L**

A suspension of compound **L²** (0.48 g, 1 mmol) in acetic acid (2 mL) was added to a stirring solution of azo-coupled precursors, **L¹**, (2 mmol) in Ethanol (25 mL) during a period of 10 min at 80 °C (see supporting information). The mixture was refluxed for 15 h at 80 °C with stirring and then was filtered whilst hot and the obtained solid was washed with hot ethanol (three time) and then with diethylether. The resulted product was dried in air. Yield: 85.7 %, m.p 206 °C. ¹H NMR (d₆-DMSO, ppm): δ 1.20 (t, 6H), 2.65 (q, 4H), 4.39 (s, 4H), 7.12 (br, s, 1H), 7.15 (br, s, 1H), 7.24 (br, m, 3H), 7.37 (dd, 5H, J=8.1), 7.77 (dd, 4H, J=8.1), 7.81 (d, 4H, J=4.58), 7.98 (br, dd, 2H), 8.33 (br, m, 2H), 8.69 (d, 4H, J=4.58), 8.97 (s, 2H), 11.43 (br, 2H). IR (KBr, cm⁻¹): 1602 (C=N), 1433 (N=N), 1263 (C-O), 1217 (N-N), 841 (C-S) and 829 (NCN_{triazole ring}). Anal. Calcd. for C₅₂H₄₄N₁₄O₂S₂.H₂O: C, 64.98; N, 20.40; H, 4.61; S, 6.67. Found: C, 64.8; N, 20.2; H, 4.3; S, 6.2%.

3. Result and discussion

3.1. Characterization

The IR spectrum of **H₂L** containing stretching bands at 1616, 1433 cm⁻¹ which are assigned for azomethine, N=N and N-N bands, respectively [25,26]. The ¹H NMR spectrum of the **H₂L** contains slightly broad signals in the region 11.58 ppm assigned to OH protons (Table 3), as were confirmed by deuterium exchange when D₂O was added to d₆-DMSO solution. The CH=N imine protons exhibit a singlet resonance in the region 8.96 ppm. Electronic absorption spectra of the **H₂L** recorded in DMSO, display mainly two bands, Table 1 and Fig. 2. The first band located at 320–393 nm corresponds to π-π* transition involving the π-electrons of the azo and azomethine groups [42]. The broad band observed

in the range 410–516 nm can be assigned to an intramolecular charge transfer interaction involving the whole molecule of dye, especially for azo groups.

Figure 2

3.2. Solvent effect on absorption spectra of the dyes

To evaluate the intermolecular forces between solvents and solute molecules, we carried out a preliminary study of the absorption spectra for prepared dye in selected solvents of different solvation character (DMSO, THF and 1,4-dioxane) at room temperature, Fig. 2. The results are given in Table 1. On the base of Kamlet–Taft parameters [43], it was found that the absorption band at 320–393 nm generally shows bathochromic shift (positive solvatochromism) as the polarity of solvent was increased. The influence of solvents for the prepared dye increases in the order DMSO > THF > 1,4-dioxane.

Table 1

3.3. Electrochemistry of H_2L

To obtain a deeper insight into the ground state properties and more specifically the mutual donor–acceptor electronic influence of ethyl group, we studied the redox properties of the H_2L by cyclic voltammetry (Figure 3). The azo-azomethine compound (H_2L) two irreversible peaks were showed. The irreversible anodic peak in the potential of + 0.85 V (vs. Calomel) may be assigned to the irreversible oxidation of the triazole moiety [44]. Also, the H_2L displayed an irreversible reduction peak in the potential of -0.67 V (vs Calomel). This peak can be attributed to the reduction of the azo compounds to hydrazone derivatives [45].

Figure 3

The cyclic voltammogram of dye was recorded at six different scan rates. The reduction and oxidation peaks are mostly dependent upon the scan rate. As the scan rate is increased the wave height increased and shift to positive and/or negative potential. Moreover, the irreversible nature of the reduction processes of azo groups was confirmed from the shift of the wave potentials to more negative values on increasing the scan rate [46].

3.4. Thermal properties

In order to give more insight into the structure of the prepared dye, the thermal study of **H₂L** has been carried out using thermogravimetry techniques. In the present investigation, the heating rates were suitably controlled at 10 °C min⁻¹ under N₂ atmosphere and the weight loss was measured from 25 °C up to 700 °C.

The initial decomposition and inflection temperatures have been used as an indication on the thermal stability of the prepared compound. The TG result indicates that the framework of dye is stable up to 245 °C, Figure 4, Table 2.

Table 2

Figure 4

The presence of water or solvent molecules in the lattice of the dye is supported by the results of thermogravimetric analysis. The first stage of mass loss is observed between 25–221 °C which is in agreement with the calculated values for the removal of water molecule from the compound.

3.5. Computational results of ¹H NMR study

The calculations for three possible tautomers of **H₂L** (see supporting information) done by undertaking a full geometry optimization at the B3LYP/6-311+G(d) level of theory.

Table 3

The ^1H NMR chemical shifts of all hydrogens for most stable tautomer, azo tautomer, were calculated on the optimized structures of compounds using GIAO/DFT method and CSGT/DFT method with 6-311+ G(d) basis set for all atoms. Calculated and measured ^1H chemical shifts of all hydrogens are tabulated in Table 3. The correlations between experimental and computed chemical shifts of hydrogens are shown in Fig. 5. The correlations are linear and they are described by the equation:

$$\delta_{\text{exp}} = \mathbf{a} + \mathbf{b} \delta \quad (2)$$

a and **b** are:

$$\delta_{\text{H}} = -0.8775 \delta + 31.9460 \quad (R^2 = 0.9882); \text{ for GIAO method}$$

$$\delta_{\text{H}} = -0.6296 \delta + 29.1010 \quad (R^2 = 0.9792); \text{ for CSGT method}$$

The small errors in the calculations toward experimental data can be due to existence equilibriums between three possible tautomers in solution.

Figure 5

3.6. Electronic structure and Natural Bonding Orbital (NBO) Analysis

The calculated electronic spectra of three stable tautomers of H_2L in DMSO are represented in Table 4. The theoretical spectra have been obtained by a TD-DFT treatment with taking into account the solvent effect, at the 400-500 nm regions. For azo, hydrazone and enammine tautomers the position of calculated electronic transitions are 479.34-479.06, 446.07- 444.51 and 449.28 nm, respectively (*see supporting information*). Among the tautomers considered in the present work, the azo tautomer has the best agreement to experimental data (Table 4) and is suggested to be the most populated one in experiment. The little errors between theory and experiment originates from (i) the temperature effects, which are only partly included in our solvation model; (ii) the vibrational effects that are not

taken into account; (iii) more essentially, the fact that PCM does not explicitly take into account H-bonds; and (iv) surely, the existence various tautomeric forms of the compound in solution.

Table 4

To shed more light on the nature and origin of the observed transitions, we conducted NBO calculation for most stable tautomer in solution, azo tautomer (Table 5). Some strong intramolecular interactions, which are formed mostly by the overlap between $n(N-N)$ and $\sigma^*(C-N)$, $\sigma^*(N-N)$, $\pi^*(C-N)$ and $\pi^*(N-N)$ bond orbital in the azo and azomethine groups, which leads intramolecular charge transfer (ICT) causing stabilization of the system have revealed by the NBO analysis.

Table 5

The strong intramolecular hyperconjugative interaction of the lone pair to σ and π electrons of the azo moieties results to stabilization of azo tautomer as evident from Table 5. Such as, the intramolecular hyperconjugative interaction of the $LP(N_{93})$ distribute to $\pi^*(N_{92}-N_{93})$ stabilization of $65.78 \text{ kcal mol}^{-1}$. This enhanced further conjugate lone pair of nitrogen atoms with antibonding orbital $\pi^*(N_{22}-C_{24})$, $(N_{32}-N_{33})$ and $(N_{22}-C_{24})$ which results to strong delocalization of 7.40 , 6.95 and $7.09 \text{ kcal mol}^{-1}$, respectively.

3.7. Analysis of experimental data

In order to obtain some information about the stoichiometry, stability and selectivity of **H₂L** toward different two valent metal ions, we investigated the complexation of **H₂L** with Cu^{2+} , Co^{2+} , Ni^{2+} and Zn^{2+} ions spectrophotometrically in DMSO at pH=9. It was found that the addition of metal ions to the **H₂L** solution affected on absorption spectrum of the ligand. The changes in the UV-Vis spectrum of **H₂L** upon addition of Cu^{2+} , Co^{2+} , Ni^{2+} and Zn^{2+} ions are presented in Figs. 6, respectively (*see supporting information*).

The maximum wavelength of the ligand was observed at 366 nm. The maximum wavelengths of complexes were observed at 356, 348, 349 and 336 nm for Cu^{2+} , Co^{2+} , Ni^{2+} and Zn^{2+} , respectively. Notably, the CT1 band, shoulder band, at ca. 442 nm decreased gradually, and the band of ligand shift to lower wavelength simultaneously with increasing metal ions concentration. Also, the clean isobestic points at ca. 350–383 nm appear after addition of metal ions, indicating interaction between metal ions and ligand.

Figure 6

The conditional stability constants were calculated by using hard-modeling analysis of spectrophotometric-mole ratio data. The computational procedure was performed using some Matlab codes written in our laboratory. The calculated spectra profile and concentration profiles are shown in Supplementary material. The best model of complex equilibrium in solution for each metal ion was selected based on the degree of calculated fitting and experimentally recorded spectra (i.e. total residual sum of squares), the shape of spectra profiles (molar absorptivity) and meaningful concentration profiles (the non-negativity and unimodality restrictions). The stability constants values as well their standard deviation are listed in Table 6. The data show the sequence of the stability constants of complexes vary as $\text{Zn(II)} > \text{Ni(II)} > \text{Cu(II)} > \text{Co(II)}$. This may be due to different geometry tendencies of the metal ions. The high stability constants of ML and ML₂ for zinc and nickel complexes, respectively, makes **H₂L** superior as a suitable ligand for developing an analytical method for selective determination of zinc and nickel ions.

Table 6

Conclusion

Synthesis, FT-IR, ¹H NMR and UV–Vis data of new acyclic 1,2,4-triazole-based azo-azomethine dye, **H₂L**, is reported. The ¹H NMR chemical shifts of azo tautomer of **H₂L** in

DMSO solution was also systematically studied by GIAO/DFT and CSGT/DFT methods at B3LYP/6-311++G(d) basis set. The GIAO/DFT computed magnetic isotropic shielding tensors correlate better with the experimental data than the CSGT/DFT ones. Moreover, the conditional stability constants were calculated by using hard-modeling analysis of spectrophotometric-mole ratio data. The data show the sequence of the stability constants of Cu^{2+} , Co^{2+} , Ni^{2+} and Zn^{2+} complexes of H_2L vary as $\text{Zn(II)} > \text{Ni(II)} > \text{Cu(II)} > \text{Co(II)}$. This may be due to different geometry tendencies of the metal ions. The high stability constants of ML and ML₂ for zinc and nickel complexes, respectively, makes H_2L superior as a suitable ligand for developing an analytical method for selective determination of zinc and nickel ions. Also, The TD-DFT and NBO studies showed that the azo tautomer are more stable in DMSO solution and the UV-Vis band at 466 nm can be assigned to transition band from lone pair of nitrogens, in azo groups, to π^* and σ^* of azo, azomethine and phenol moieties.

Acknowledgments

We are grateful to the Arak University for financial support of this work.

Reference

- [1] A. Vig, K. Sirbiladze, H.J. Nagy, P. Aranyosi, I. Rusznák, P. Sallay, *Dyes Pigments* 71 (2006) 199–205.
- [2] M.M.M. Raposo, A.M.R.C. Sousa, A.M.C. Fonseca, G. Kirsch, *Tetrahedron* 61 (2005) 8249–8256.
- [3] A.T. Slark, P.M. Hadgett, *Polymer* 40 (1999) 4001–4011.
- [4] G. Hallas, J.H. Choi, *Dyes Pigments* 40 (1999) 119–129.
- [5] M.S. Ho, A. Natansohn, P. Rochon, *Macromolecules* 28 (1995) 6124–6127.
- [6] Y. Nabeshima, A. Shishido, A. Kanazawa, T. Shiono, T. Ikeda, T. Hiyama, *Chem. Mater.* 9 (1997) 1480–1487.

- [7] G. Iftime, F.L. Labarthe, A. Natansohn, P. Rochon, K. Murti, *Chem. Mater.* 14 (2002) 168–174.
- [8] S.M. Ghoreishi, R. Haghghi, *Chem. Eng. J.* 95 (2003) 163–169.
- [9] Y.M. Song, Y.M. Ha., J.A. Kim, K.W. Chung, Y. Uehar, K.J. Lee, P. Chun, Y. Byun, H.Y. Chung, H.R. Moon, *Bioorg. Med. Chem. Lett.* 22 (2012) 7451-7455.
- [10] C. Hsu, T.N. Wen, Y.C. Su, Z.B. Jiang, C.W. Chen, L.F. Shyur, *Environ. Sci. Technol.* 46 (2012) 5109–5117.
- [11] A.M. Khedr, M. Gaber, R.M. Issa, H. Erten, *Dyes Pigments* 67 (2005) 117–126.
- [12] M. Gaber, Y.S. El-Sayed, K. El-Baradie, R.M. Fahmy, *J. Mol. Struct.* 1032 (2013) 185-194.
- [13] B. Hu, G. Wang, W. You, W. Huang, X.Z. You, *Dyes Pigments* 91 (2011) 105–111.
- [14] X.Y. Li, Y.Q. Wu, D.D. Gu, F.X. Gan, *Mater. Sci. Eng., B* 158 (2009) 53–57.
- [15] R. Gup, E. Giziroglu, B. Kırkan, *Dyes Pigments* 73 (2007) 40–46.
- [16] S. Wang, S. Shen, H. Xu, *Dyes Pigments* 44 (2000) 195-198.
- [17] M.S. Refat, I.M. El-Deen, H.K. Ibrahim, S. El-Ghool, *Spectrochim. Acta, Part A* 65 (2006) 1208–1220.
- [18] K. Nejati, Z. Rezvani, B. Massoumi, *Dyes Pigments* 75 (2007) 653-657.
- [19] H. Dincalp, F. Toker, I. Durucasu, N. Avcıbaşı, S. Icli, *Dyes Pigments* 75 (2007) 11-24.
- [20] Z. Rezvani, A.R. Abbasi, K. Nejati, M. Seyedahmadian, *Polyhedron* 24 (2005) 1461–1470.
- [21] L.D. Popov, Y.P. Tupolova, V.V. Lukov, I.N. Shcherbakov, A.S. Burlov, S.I. Levchenkov, V.A. Kogan, K.A. Lyssenko, E.V. Ivannikova, *Inorg. Chim. Acta* 362 (2009) 1673–1680.
- [22] X. Li, Y. Wu, D. Gu, F. Gan, *Dyes Pigments* 86 (2010) 182-189.

- [23] S. Brooker, *Coord. Chem. Rev.* 222 (2001) 33–56.
- [24] J.G. Haasnoot, *Coord. Chem. Rev.* 200–202 (2000) 131–185.
- [25] H. Khanmohammadi, M. Erfantalab, *Spectrochim. Acta, Part A* 86 (2012) 39–43.
- [26] H. Khanmohammadi, M. Erfantalab, A. Bayat, A. Babaei, M. Sohrabi, *Spectrochim. Acta, Part A* 97 (2012) 876–884.
- [27] C.D. Brant, J.A. Kitchen, U. Beckmann, N.G. White, G.B. Jameson, S. Brooker, *Supramol. Chem.* 19 (2007) 17–27.
- [28] M.H. Klingele, B. Mobaraki, K.S. Murray, S. Brooker, *Chem. Eur. J.* 11 (2005) 6962–6973.
- [29] J.A. Kitchen, S. Brooker, *Coord. Chem. Rev.* 252 (2008) 2072–2092.
- [30] C.J. McHugh, F.T. Docherty, D. Graham, W.E. Smith, *Analyst* 129 (2004) 69–72.
- [31] A. Enright, L. Fruk, A. Grondin, C.J. McHugh, W.E. Smith, D. Graham, *Analyst* 129 (2004) 975–978.
- [32] R. Ditchfield, *Mol. Phys.* 27 (1974) 789–807.
- [33] K. Wolinski, J.F. Hinton, P. Pulay, *J. Am. Chem. Soc.* 112 (1990) 8251–8260.
- [34] T.A. Keith, R.F.W. Bader, *Chem. Phys. Lett.* 194 (1992) 1–8.
- [35] T.A. Keith, R.F.W. Bader, *Chem. Phys. Lett.* 210 (1993) 223–231.
- [36] R.E. Stratmann, G.E. Scuseria, M.J. Frisch, *J. Chem. Phys.* 109 (1998) 8218–8224.
- [37] M.J. Frisch, G.W. Trucks, H.B. Schlegel, G.E. Scuseria, M.A. Robb, J.R. Cheeseman, J.A. Montgomery, J.T. Vreven, K.N. Kudin, J.C. Burant, J.M. Millam, S.S. Iyengar, J. Tomasi, V. Barone, B. Mennucci, M. Cossi, G. Scalmani, N. Rega, G.A. Petersson, H. Nakatsuji, M. Hada, M. Ehara, K. Toyota, R. Fukuda, J. Hasegawa, M. Ishida, T. Nakajima, Y. Honda, O. Kitao, H. Nakai, M. Klene, X. Li, J.E. Knox, H.P. Hratchian, J.B. Cross, C. Adamo, J. Jaramillo, R. Gomperts, R.E. Stratmann, O. Yazyev, A.J. Austin, R. Cammi, C. Pomelli, J.W. Ochterski, P.Y. Ayala, K. Morokuma, G.A. Voth,

P. Salvador, J.J. Dannenberg, V.G. Zakrzewski, S. Dapprich, A.D. Daniels, M.C. Strain, O. Farkas, D.K. Malick, A.D. Rabuck, K. Raghavachari, J.B. Foresman, J.V. Ortiz, Q. Cui, A.G. Baboul, S. Clifford, J. Cioslowski, B.B. Stefanov, G. Liu, A. Liashenko, P. Piskorz, I. Komaromi, R.L. Martin, D.J. Fox, T. Keith, M.A. Al-Laham, C.Y. Peng, A. Nanayakkara, M. Challacombe, P.M.W. Gill, B. Johnson, W. Chen, M.W. Wong, C. Gonzalez, J.A. Pople, Gaussian 03, Gaussian Inc., Pittsburgh, PA, USA, 2003.

[38] Hyper Chem. Release 5.02, Hypercube, Inc., Gainesville, 1997.

[39] J. Tomasi, B. Mennucci, R. Cammi, *Chem. Rev.* 105 (2005) 2999-3093.

[40] J.P. Foster, F.J. Weinhold, *Am. Chem. Soc.* 102 (1980) 7211-7218.

[41] A.E. Reed, L.A. Curtiss, F. Weinhold, *Chem. Rev.* 88 (1988) 899-926.

[42] N.M. Rageh, *Spectrochim. Acta Part A* 60 (2004) 103–109.

[43] (a) S. Ichijima, H. Kobayashi, *Bull. Chem. Soc. Jpn.* 78 (2005) 1929–1938; (b) M.R. Mahmoud, S.A. Ibrahim, M.A. Hamed, *Spectrochim. Acta, Part A* 39 (1983) 729-733.

[44] S. Brillians Revin, S. Abraham John, *Electrochimic. Acta* 56 (2001) 8934-8940.

[45] Z. Mandić, B. Nigović, B. Šimunić, *Electrochimic. Acta* 49 (2004) 607-615.

[46] M. M. Ghoneim, H. S. El-Desoky, S. A. Amer, H. F. Rizk, A. D. Habazy, *Dyes and Pigments* 77 (2008) 493-501.

Table 1. Absorption spectral data of **H₂L** in various solvents.

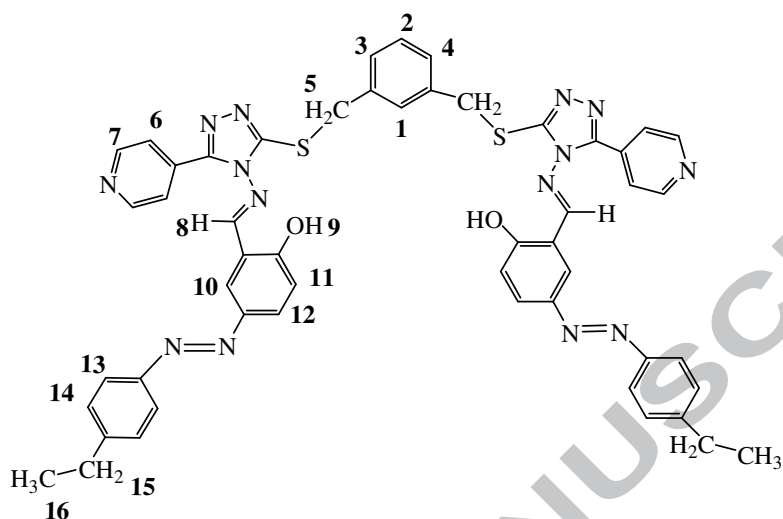
Solvent	λ_{\max}/nm ($\epsilon \times 10^3/\text{M}^{-1} \text{cm}^{-1}$)
DMSO	344(44.0)
	466(10.1)
1,4-Dioxane	339(58.9)

THF	336(55.7)

Table 2: Thermal analyses data for **H₂L**

Compound, M.F. (M. Wt.)	Dissociation Stages	Temperature range in TG (°C)	Weight loss, Found (Calculated) (%)	Proposed decomposition assignment	T _d (°C)
H₂L , C ₅₂ H ₄₄ N ₁₄ O ₂ S ₂ (961.13)	Stage I	25-121	1.8 (1.84)	The loss of 1 molecule H ₂ O	245
	Stage II	121-284	28.4 (28.41)	The loss of C ₉ H ₇ N ₉ S	
	Stage III	284-378	36.5 (36.47)	The loss of C ₉ H ₉ N ₅ O ₂ S	
	Stage IV	378-700	----	The loss of remaining parts	

Table 3: Selected hydrogen chemical shifts (δ , ppm) in d_6 -DMSO and calculated magnetic isotropic shielding tensors for more stable isomer of H_2L .



Atoms	experimental	GIAO/DFT	CSGT/DFT
H ₁	7.12	25.9450	24.879
H ₂	7.15	25.4550	24.5249
H ₃	7.22	25.7295	24.6533
H ₄	7.24	25.1098	24.412
H ₅	4.39	28.1650	26.1416
H ₆	7.81	24.6805	23.9977
H ₇	8.69	24.3933	23.1972
H ₈	8.97	24.093	23.7557
H ₉	11.43	23.5268	25.4932
H ₁₀	8.33	24.7009	24.1737
H ₁₁	7.32	25.7706	24.3438
H ₁₂	8.01	24.9848	24.0817
H ₁₃	7.77	25.2356	24.2402
H ₁₄	7.37	25.3533	24.4534
H ₁₅	2.65	29.4824	27.5124
H ₁₆	1.20	31.0495	28.3982

Table 4: Calculated optical transitions ($f > 0.04$) for **H₂L** tautomers in DMSO at B3LYP/6-311+g(d).

Tautomer	λ (nm)	Predominant transitions	f^d	Contribution (%)
a	479.34	HOMO→LUMO+1	0.1510	5.28
		HOMO→LUMO+3		12.08
		HOMO-1→LUMO		16.75
		HOMO-1→LUMO+3		2.54
		HOMO-1→LUMO+2		37.54
	479.06	HOMO→LUMO+1	0.0562	16.58
		HOMO→LUMO+2		2.68
		HOMO→LUMO+3		37.63
		HOMO-1→LUMO+2		11.91
	409.54	HOMO→LUMO+1	0.1042	3.57
		HOMO-1→LUMO		60.84
		HOMO-1→LUMO+1		2.44
HOMO-1→LUMO+2		23.16		
b	446.07	HOMO-1→LUMO	0.6354	58.86
		HOMO-2→LUMO		19.09
		HOMO→LUMO+1		9.09
	444.51	HOMO→LUMO+1	0.6940	58.24
		HOMO-1→LUMO		9.09
		HOMO-2→LUMO+1		4.54
c	494.46	HOMO-1→LUMO	0.3878	31.45
		HOMO-1→LUMO+2		15.13
		HOMO→LUMO+1		18.63
	493.81	HOMO→LUMO+1	0.0811	30.69
		HOMO→LUMO+3		15.63
	449.28	HOMO→LUMO+3	0.0174	43.63

^a azo tautomer; ^b hydrazone tautomer; ^c enaminone tautomer; ^d oscillator strength; ^e Intramolecular charge transfer

Table 5: Second-order perturbation theory analysis of Fock matrix on NBO basis for most stable tautomer of H_2L , azo tautomer, by using B3LYP/6-311+g(d).

Donor(<i>i</i>)	Occupancy (ED/e)	Acceptor(<i>j</i>)	Occupancy (ED/e)	$E(2)^a$ (Kcal/mol)	$E_j - E_i^b$ (a.u.)	$F(i,j)^c$ (a.u.)
LP(N ₃₂) ^d	1.90562	$\sigma^*(\text{N}_{33}-\text{C}_{34})$	0.05237	14.23	0.78	0.095
		$\sigma^*(\text{C}_{26}-\text{O}_{31})$	0.02106	0.90	0.40	0.017
		$\pi^*(\text{N}_{21}-\text{C}_{23})$	0.17812	2.51	0.21	0.020
		$\pi^*(\text{N}_{32}-\text{N}_{33})$	0.14248	6.95	0.16	0.030
LP(N ₃₃)	1.89829	$\sigma^*(\text{N}_{32}-\text{C}_{29})$	0.05378	18.13	0.57	0.092
		$\pi^*(\text{N}_{32}-\text{C}_{29})$	0.38861	7.09	0.40	0.052
LP(N ₉₂)	1.90600	$\pi^*(\text{N}_{22}-\text{C}_{24})$	0.17609	7.40	0.31	0.046
		$\pi^*(\text{N}_{92}-\text{N}_{93})$	0.14235	3.65	0.14	0.021
		$\sigma^*(\text{N}_{92}-\text{N}_{93})$	0.01273	5.51	0.73	0.058
LP(N ₉₃)	1.89734	$\pi^*(\text{N}_{22}-\text{C}_{24})$	0.17609	1.87	0.93	0.026
		$\pi^*(\text{N}_{92}-\text{N}_{93})$	0.14235	65.78	0.14	0.087
		$\sigma^*(\text{N}_{92}-\text{N}_{93})$	0.01273	2.05	0.90	0.039

^a $E(2)$ means energy of hyper conjugative interactions (stabilization energy).

^b Energy difference between donor and acceptor *i* and *j* NBO orbitals.

^c $F(i, j)$ is the Fock matrix element between *i* and *j* NBO orbital.

^d LP(A) is a valence lone pair orbital on A atom.

Table 6. Results of $\log K_\beta$ for Metal-Ligand Complexes ^a

Metal / Ligand	$\log K_\beta$	Metal / Ligand	$\log K_\beta$
Cu ²⁺	ML	Ni ²⁺	ML2
	ML2		M2L
	SSE ^b		SSE
Zn ²⁺	ML	Co ²⁺	ML2
	M2L		M2L
	M3L		SSE
	SSE		SSE

^a L, Schiff base; ^b SSE, Sum of Squares Errors.

Figure Captions:

Figure 1: The synthesized 1,2,4-triazole-based azo-azomethine dye (**H₂L**)

Figure 2: The electronic absorption spectra of **H₂L** (3.0×10^{-5} M) in various solvent

Figure 3: Cyclic voltammogram for **3b** (1.0×10^{-3} M) in DMSO solution with various scan rates

Figure 4: TGA/DTA of **H₂L**

Figure 5: Plot of experimental chemical shifts vs. magnetic isotropic shielding tensors from the GIAO and CSGT methods at B3LYP/6-311+G(d) calculation for most stable tautomer (azo tautomer).

Figure 6: Experimental absorption spectra for the Zn^{2+} complex with **H₂L** at pH=9. The analytical concentration of **H₂L** is 2.0×10^{-5} (mol L^{-1}), The concentrations of metal is: (1) 0.0; (2) 1.0×10^{-6} ; (3) 4.0×10^{-6} ; (4) 8.0×10^{-6} ; (5) 10.0×10^{-6} ; (6) 12.0×10^{-6} ; (7) 14.0×10^{-6} ; (8) 16.0×10^{-6} ; (9) 18.0×10^{-6} ; (10) 20.0×10^{-6} ; (11) 24.0×10^{-6} ; (12) 26.0×10^{-6} ; (13) 28.0×10^{-6} ; (14) 30.0×10^{-6} ; (15) 32.0×10^{-6} ; (16) 36.0×10^{-6} ; (17) 40.0×10^{-6} (mol L^{-1}).

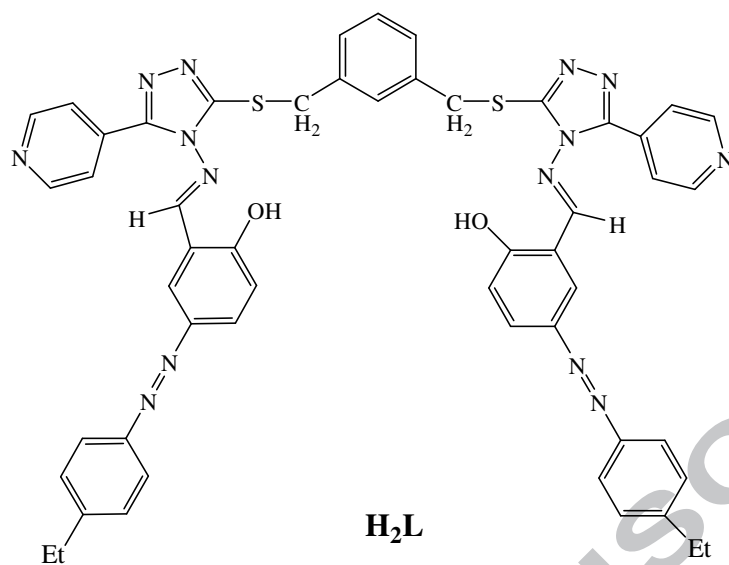


Figure 1

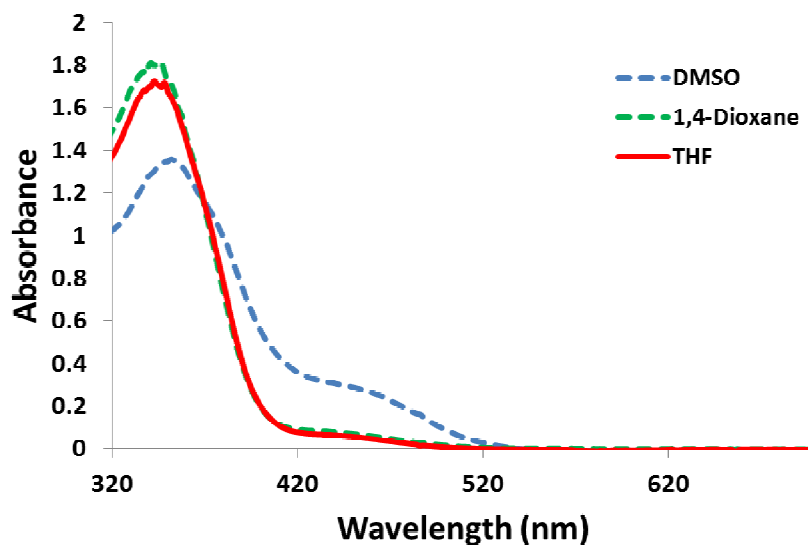


Figure 2

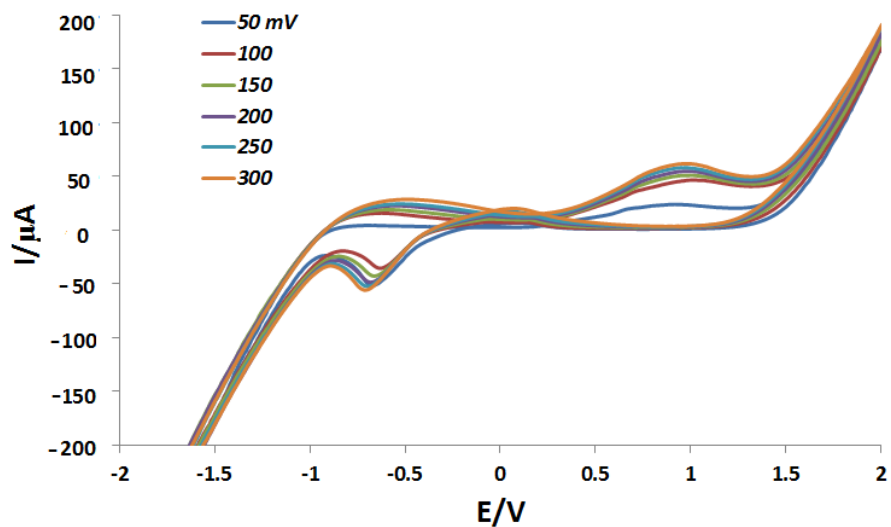


Figure 3

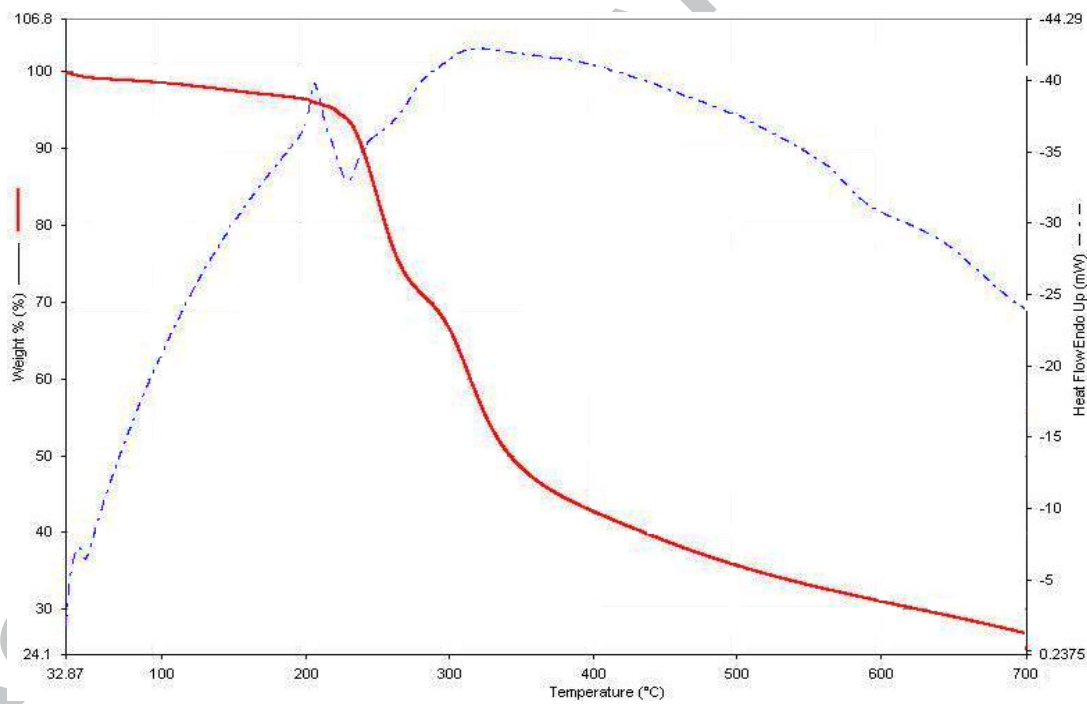


Figure 4

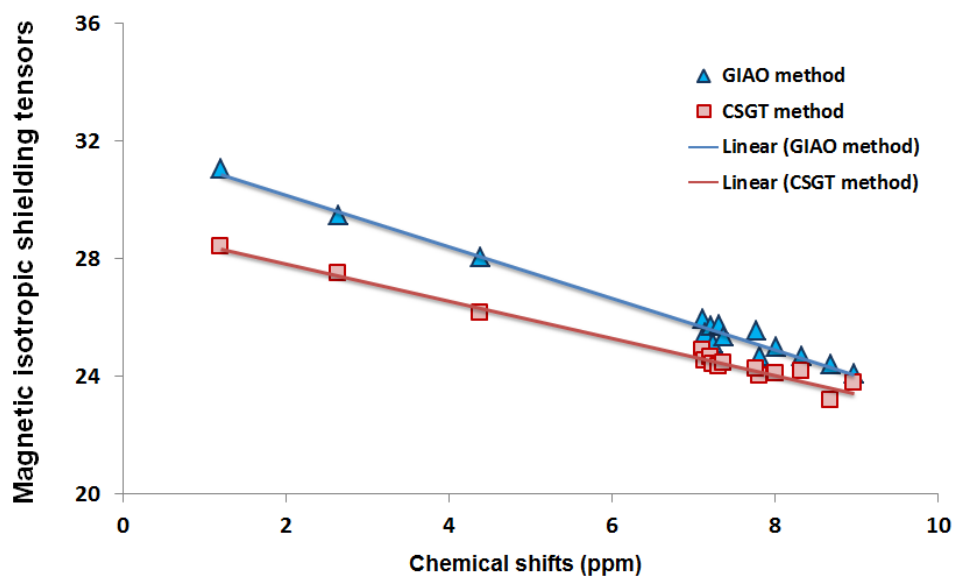


Figure 5

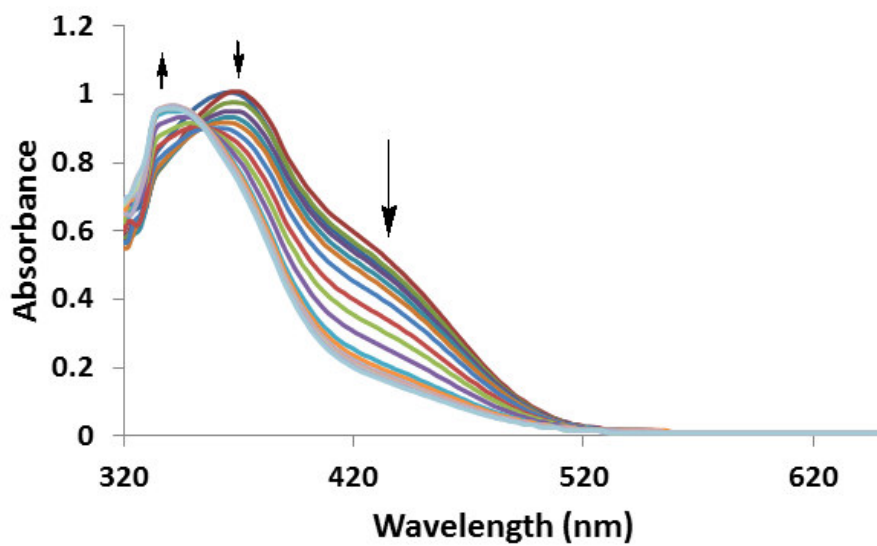
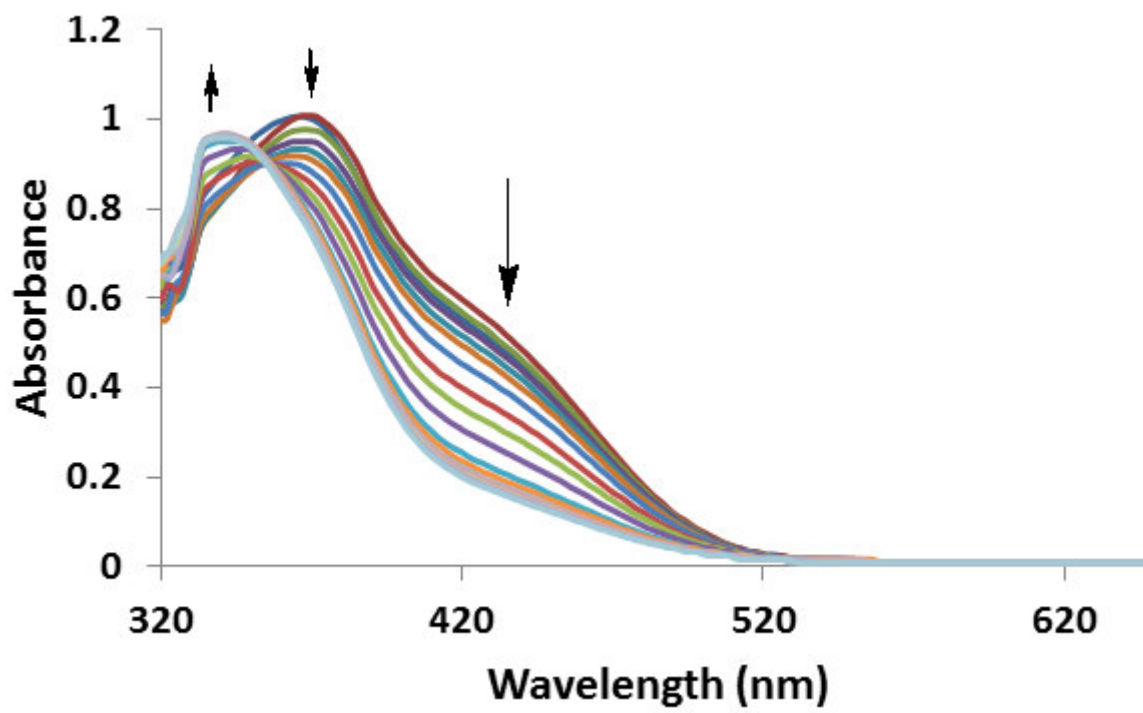


Figure 6



Highlights

- New azo-azomethine dye on base of 1,2,4-triazole has synthesized.
- The first TD-DFT and NBO studies on azo-azomethine dye have been reported.
- Hard model chemometrics method has been used to determine the formation constants of zinc(II), copper(II), nickel(II) and cobalt(II) complexes of dye in DMSO.
- The ^1H NMR chemical shifts of azo tautomer was studied by GIAO and CSGT methods at B3LYP/6-311++G(d) basis set.